Strain Measurements In Thermally Loaded Circuit Boards Containing Embedded Resistors

E. S. Drexler, R. C. Snogren*, M. C. Snogren*, J. J. Felten**, P. A. Green***
National Institute of Standards and Technology
325 Broadway, Materials Reliability Division
Boulder, CO 80305
drexler@boulder.nist.gov

*SAS Circuits, Inc.
10570 Bradford Rd.
Littleton, CO 80127

**DuPont Technologies
14 T.W. Alexander Dr.
Research Triangle Park, NC 27709-4425

***Coretec Inc.
2020 Ellesmere Rd.
Scarborough, Ontario, CANADA M1H 2Z8

Abstract

Four specimens of embedded resistors were tested from room temperature to the processing temperature (177 °C) to compare deformations in the printed wiring board (PWB) by means of electron-beam moiré. The specimens had different termination sizes and geometries; two with straight approaches to the termination came from one board, and three with indirect approaches came from a second board. In none of the specimens did deformation occur in the embedded resistor or at the interface between the resistor and the termination. However, significant deformation occurred within the PWB and the laser barrier of the specimens with the indirect approach to the termination. Strains as high as 6 % were calculated in areas of that PWB. And in two specimen, the mismatch in thermal expansion between the resistor and the laser barrier was so great that a crack developed at that interface.

Introduction

Improved performance and lighter, more compact consumer electronics are motivating the microelectronics industry to incorporate embedded passive components into the printed wiring board (PWB). Shorter lead lengths and reduced inductance improve the efficiency and performance [1]. Since passive components can make up 90 % of the devices on the PWB of a typical cell phone [1], large improvements in size and weight reduction can be realized by embedding many of those passive components.

There are trade-offs when it comes to reliability of embedded versus discrete passives; eliminating solder joints should improve the reliability of the components if flexure of the PWB can be minimized or the passives be made sufficiently elastic to prevent cracks from forming. Other reliability issues might include aging, interfacial integrity, accuracy of deposition, and mismatches in thermal expansion. Thermal-expansion mismatches are manifested by strain concentrations that can result in failures due to interfacial cracking or fatigue. Measurement of thermally induced strains will identify strain concentrations, and, therefore, possible failure sites.

Using electron-beam moiré, we compared four different geometries of interconnects and terminations to an embedded resistor, to determine which geometry will best mitigate the strains in the board at the processing temperature (177 °C). Electron-beam moiré relies on the same principles as geometric or optical moiré, whereby the interference between two similarly pitched gratings produces moiré fringes. The reference grating, in the case of electron-beam moiré, is the raster of the electron beam in the scanning electron microscope (SEM), which rasters at a very regular rate and interval, allowing for reproducible generation of moiré fringes [2,3]. Please see references 2–5 for further descriptions of the technique and its application to microelectronics packaging.

The choice of a ceramic resistor material was based on the fact that ceramic chip resistors are the current industry standard for surface-mounted resistive components. The ceramic materials are processed at much higher temperatures than polymer-based resistive pastes, and will readily tolerate high temperatures such as those encountered during soldering operations, whereas polymer-based materials are more problematic. The need to fire them on copper foil limits the choice of materials to those compatible with nitrogen firing. Resistors based on a conductive phase of lanthanum hexaboride (LaB_6) are such a material system, which is currently in widespread use on ceramic substrates in the industry [6].

The flow chart and schematics in Figure 1 show the process for manufacturing the PWBs incorporating the embedded resistors. The ceramic resistor requires a processing temperature of 177 °C. During the innerlayer process and the final multi-layer board (MLB) lamination

process, the resistor and surrounding materials are heated to 177 °C for approximately one hour each time with a controlled ramp up and down. The FR-4 core is laminated into a multilayer PWB using conventional MLB materials and processes. The epoxy employed in the PWB is that used for standard FR-4 PWBs at the manufacturer and has a glass transition temperature of 170 °C. Interconnections may be made with through vias or microvias.

Experiment

Specimens from two different boards were tested to determine whether changing the geometry of the resistor terminations would mitigate thermally induced strains near the embedded resistors. Neither board had any active or passive discrete components attached. On one board the interconnect approach to the termination was direct, and the terminations had two different lengths, approximately 0.25 mm and 0.5 mm. The other board had indirect approaches to the terminations; that is, there were two 90° bends in the interconnect before reaching the termination. A total of five specimens, two from the first board and three from the second, were tested; two from each board originated from the same locations. Each specimen comprised a series of nine pairs of terminations connected by resistors composed of LaB_6. Figure 2 shows a schematic of the diverse materials contained in the images collected during the thermal loading. The laser barrier, a TiO_2 filled epoxy, was needed to protect the substrate during laser trimming of the resistor. The metal, ceramic, and filled polymers have vastly differing coefficients of thermal expansion (CTE), which can contribute to strain concentrations and, ultimately, fracture or fatigue.

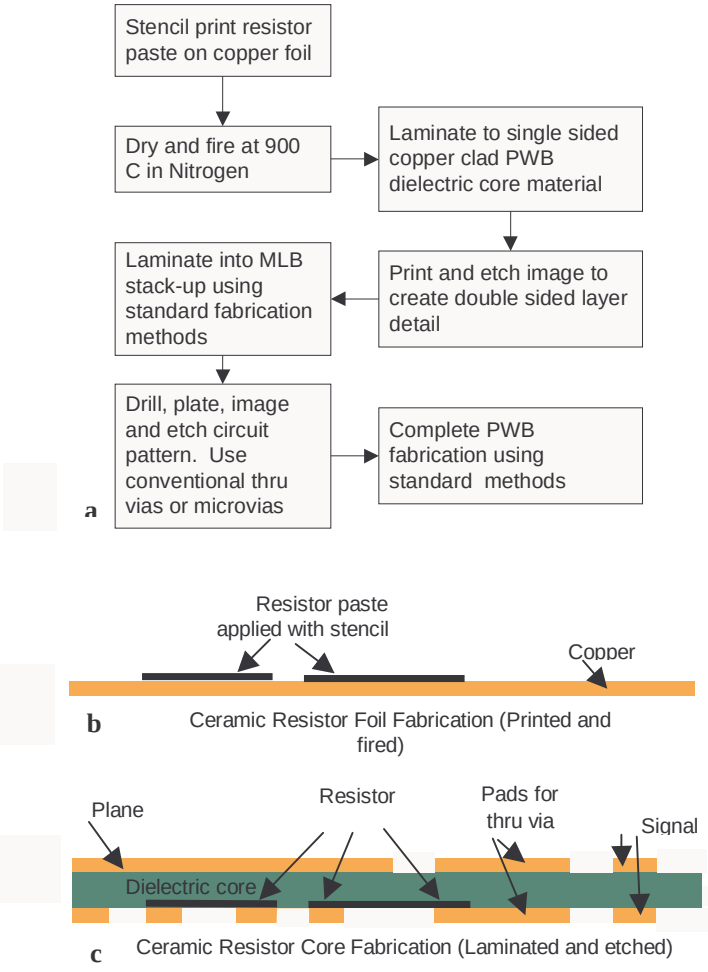

Figure 1. Flow chart (a) showing the manufacturing process for embedding ceramic resistors in PWB. Schematics (b) and (c) correspond to the process steps shown in frames 1 and 4, respectively, of the flow chart.

Electron-beam moiré was employed to determine strains in the five specimens at 177 °C and after cool-down to room temperature (~27 °C). A quantitative technique, electron-beam moiré measures *u*-field and *v*-field displacements from which normal and shear strains may be calculated (eg., $\varepsilon_x = \partial u/\partial x$, or the slope of a curve of displacement versus position). The resolution of the displacement measurements is proportional to the line pitch of the specimen grating and the quality of the fringe field. For these tests, moiré crossed-line gratings with 450 or 175 nm line pitches were instrumented onto the cross-sectioned and polished surfaces of the specimens at regular intervals across the section. The interference between the specimen grating and the raster of the electron beam generates a fringe field. Each specimen was individually heated from room temperature to 177 °C in 30 °C increments and images recorded from 1 to 3 locations, then cooled to room temperature, at which time final images were recorded. The images from the thermally loaded and final images were compared with the initial unloaded, room-temperature image so that changes in the fringe field could be determined with respect to temperature. The changes in the fringe field relate to displacement through the equation $(u,v) = \Delta N_f \, p_r$. For the images from these tests, higher density of fringes indicates tension, and a lower density of fringes indicates compression.

Results

A general comparison between the two boards showed that more strain was induced at 177 °C in the boards with the indirect interconnects. In all cases, the highest strains were generated within the epoxy-rich regions of the glass-fiber-reinforced epoxy. Figure 3 shows the initial-condition images, the moiré images acquired at 177 °C, and the curves of displacement versus position from the indicated location

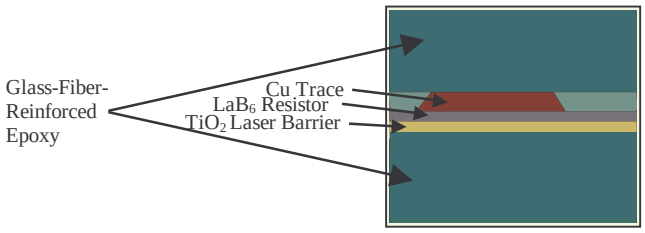

Figure 2. Schematic showing the relative locations of the materials contained in a typical moiré images.

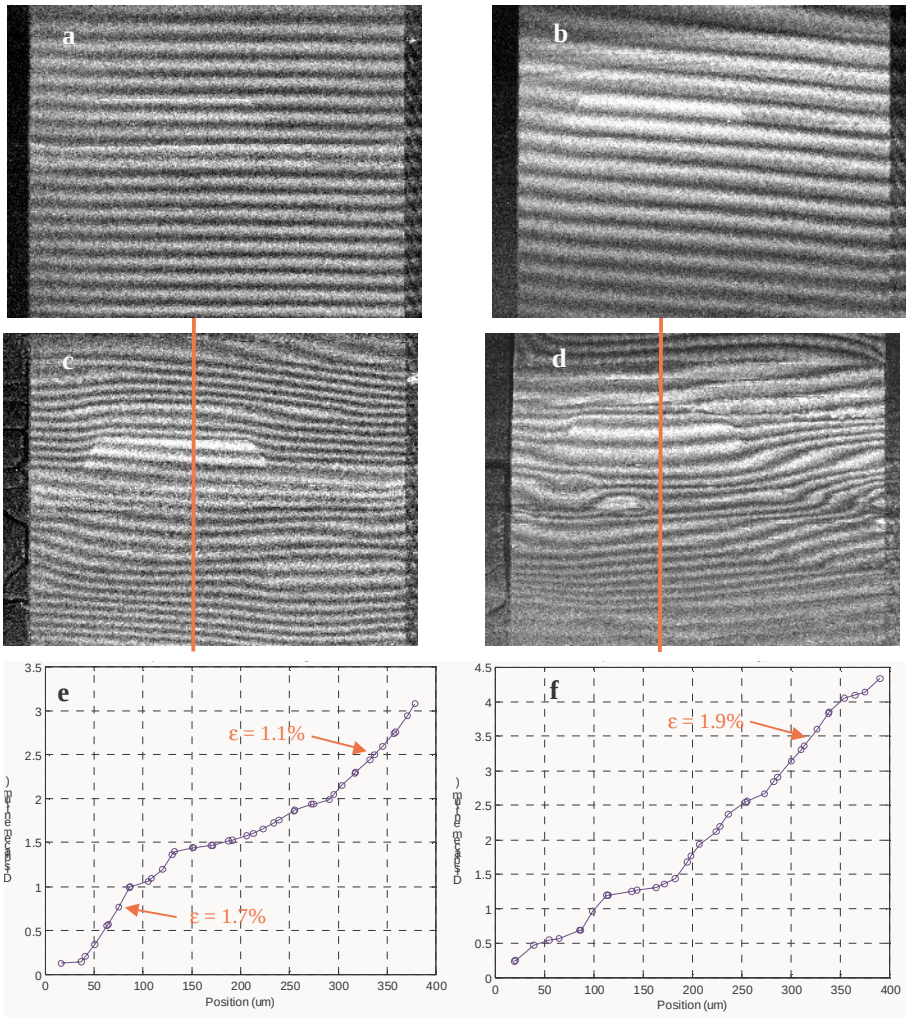

Figure 3. Moiré images from the same location and geometry from the two different boards at room temperature prior to thermal loading (a and b), the corresponding images at 177 °C (c and d), and the graphs of displacement versus position (e and f) for the respective line profiles indicated in c and d. Note the difference in the magnitude of the displacement scales.

from the two boards at approximately the same site, grating pitch, and orientation. Furthermore, this same board exhibited greater permanent deformation at the end of the test at room temperature (Figure 4). Strains as large as 8 % or more at 177 °C were observed elsewhere in the PWB with the indirect interconnects. The board that contained the direct interconnects displayed lesser amounts of strain in the glass-fiber-reinforced epoxy, around 2 %, and less permanent deformation at the end of the test. A comparison between the long termination and the shorter termination of the direct interconnects at room temperature, prior and subsequent to thermal loading, showed that the 0.5-mm termination recovered from thermal loading virtually strain-free (Figure 5). All geometries displayed large mismatches in thermal expansion that resulted in strain concentrations between the resistive layer and the TiO_2 laser barrier, and in the resin-rich areas around the termination. In two specimens a crack formed to relieve that strain concentration between the resistive layer and the TiO_2 laser barrier. Figure 6 shows two of the locations, just before and after the cracks formed. Cracks are evinced by the discontinuity of the moiré fringes as they cross the interface.

Figure 7 shows the preloaded and loaded (177 °C) *u*-field and *v*-field images from the second board. These images clearly illustrate the anisotropic behavior of the glass-fiber-reinforced epoxy; the regions containing a high glass density show much less strain than the epoxy-rich regions. Strain concentrations are apparent in the TiO_2 laser barrier, in the epoxy-rich region adjacent to the Cu termination, and in various epoxy-rich locations in the glass-fiber-reinforced epoxy (encircled in Figure 7d). In the corresponding strain maps (Figures 7d and e) those areas are light blue to red [7]. From the loaded images in Figures 6 and 7, it is apparent how the strain concentrations can lead to cracks forming within the glass-fiber-reinforced epoxy and at the interface between the resistor and the laser barrier. Although it may be less obvious, another vulnerable area is at the corners of the Cu termination. The prepreg layers upon lamination allow the epoxy to flow into the open areas, specifically between the terminations. This unfilled epoxy with its very high CTE expands 6 to 8 % at high temperatures, and puts the less expansive Cu in tension (note the moiré fringes bending around the termination in Figure 7d). The CTE mismatch also makes the interface between the epoxy and the resistor susceptible to cracking; therefore, both interfaces of the resistor are in tension—from the epoxy's expansion above, and the laser barrier's expansion below.

Figure 8 shows the *u*- and *v*-field orientations of approximately the same view and magnification of the two different-sized terminations from the same board at 177 °C. In neither case are the deformations particularly large; however, they are noticeably more pronounced in the images with the shorter termination. This is especially evident at the corners of the termination where the moiré fringes scarcely curve around the longer Cu termination.

Conclusions

For all geometries and both PWBs the interface between the Cu termination and the LaB_6 resistor remained strain-free

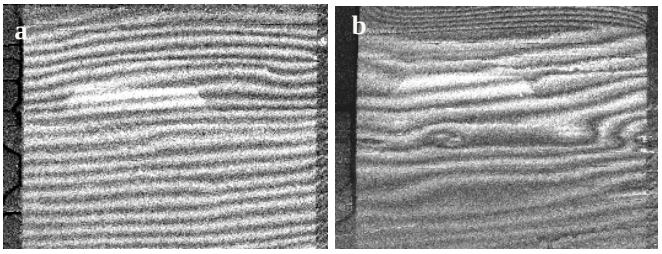

Figure 4. Final room-temperature moiré images from the same location from the two different PWBs, showing the permanent deformation brought about by thermal loading.

under thermal loading at 177 °C. Straight, continuous fringes across this interface are evidence of this strain-free condition. The amount of deformation in a given specimen did not appear to be dependent on the location on the cross section; that is, deformations were essentially uniform whether at the center or edge of the specimen. This is not unexpected, lacking the presence of any active components on the surface to introduce constraint. For specimens of the same geometry, the location on the PWB did not influence the magnitude of deformation.

Differences did exist between the two geometries from the first board, however. Specimens with the longer termination displayed less strain and had virtually complete recovery upon (thermal) unloading. The longer termination geometry leaves less space to be occupied with the unfilled epoxy. The expansion in the unfilled epoxy between the termination pairs is especially a cause for concern, as the expansion is greater above the resistor than below, generating bending, which can lead to cracking in the resistors at those locations in the PWB. This condition is present in the *v*-field images collected at 177 °C and displayed in Figures 3c and d, 6d and 7d.

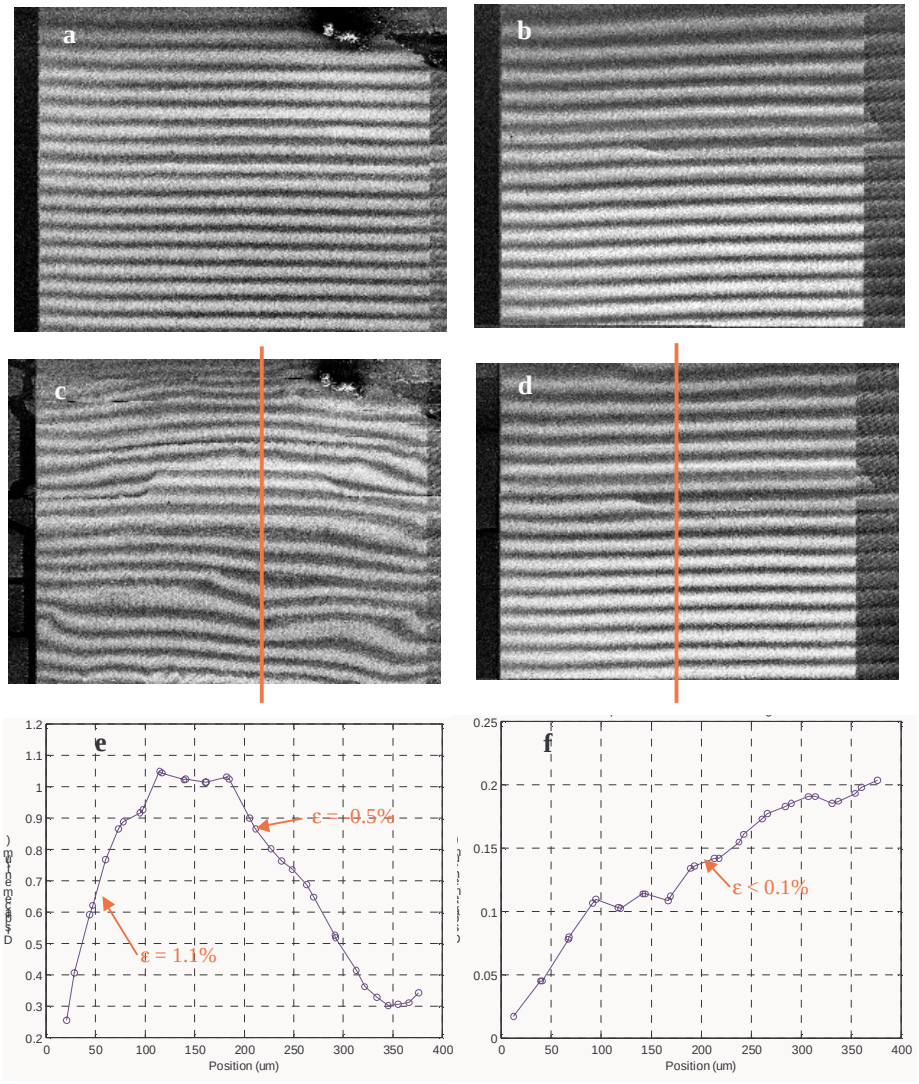

Figure 5. Moiré images from specimens with two different geometries from the same PWB are shown at room temperature for the 0.25 mm termination (a) and the 0.5 mm termination (b) prior to thermal loading, and for the 0.25 mm termination (c) and the 0.5 mm termination (d) subsequent to thermal loading. Graphs of displacement versus position are shown for the corresponding line traces in (e and f). Note the difference in magnitude of the displacement scales.

Large differences in the magnitude of strain and in the amount of permanent deformation exist between the two PWBs. In only the second PWB are cracks formed between the resistor and the laser barrier. At this time, the role played by the indirect interconnects to the terminations is unclear. Comparing the value for strain in the epoxy-rich region between the terminations shows that the strain is approximately 2 % higher in the boards with the indirect interconnects than from similar locations on the PWB with direct interconnects. Since the process and materials are the same for the two boards, then it might follow that the geometry must be responsible for the larger strains. However, the geometry of the interconnect is in the plane of the PWB, whereas, the strains being measured are through the thickness of the PWB, so the cause and effect are not apparent.

Much of the damage within the glass-fiber-reinforced epoxy is due to exceeding the glass- transition temperature of the epoxy and may be exacerbated by the free surface's lacking mechanical constraint. However, damage that could ultimately result in failure of an embedded resistor

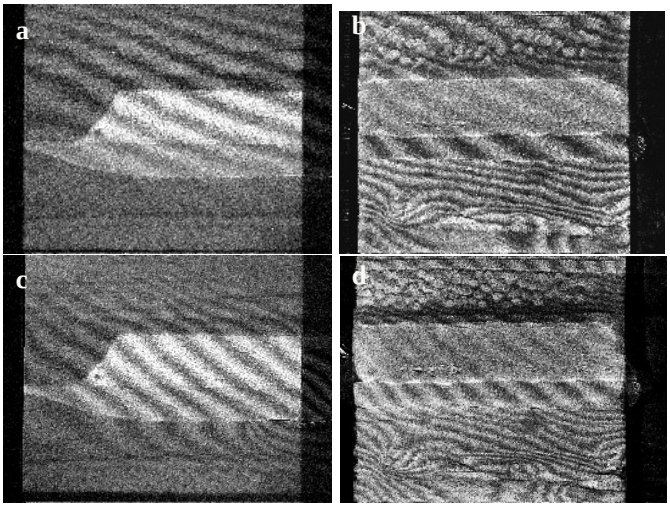

Figure 6. Moiré images from two different specimens from the same PWB. Images acquired just before the cracks formed in first specimen (a) and the second specimen (b). Images acquired after the crack had formed at the interface between the resistor and the laser barrier in the first specimen (c) and the second specimen (d).

would be probably due to strain concentrations from the unfilled epoxy between the terminations inducing cracks in the center of the resistor due to flexure, or from the combined strain in the unfilled epoxy and the TiO_2 laser barrier causing delamination at the corner of the Cu termination and the resistor.

References

1. Marcanti, L. and Dougherty, J. P., "Embedded Passives: Promising Improved Performance," *Circuits Assembly*, Vol. 12, No. 7 (2001), pp. 28–39.
2. Drexler, E. S., *Procedures for the Electron-Beam Moiré Technique*, Natl Inst Stand Technol Technical Note 1500-2 (U. S. Government Printing Office, Washington, DC, 1998), p. 133.
3. Read, D.T., and Dally, J.W., "Theory of Electron-Beam Moiré," *J Res Natl Inst Stand Technol*, Vol. 101, No. 1, (1996), pp. 47–61.
4. Drexler, E. S., "Thermally Induced Deformations in a Flip-Chip HDI Substrate," *Proc of the 50th Electronic Components and Technology Conf*, Las Vegas, NV, May 2000, pp. 650–656.
5. Drexler, E. S., "Plastic Strain in Thermally Cycled Flip-Chip PBGA Solder Bumps," *IEEE Trans on Adv Packaging*, Vol. 23, No. 4 (2000), pp. 646–651.
6. Felten, J., and Ferguson, S., "Embedded Ceramic Resistors and Capacitors for PWB," *Proc of the IPC Annual Meeting 2001*, Orlando, FL, October 2001, pp. S08-5-1–4.
7. A color version of this document is available from the first author.

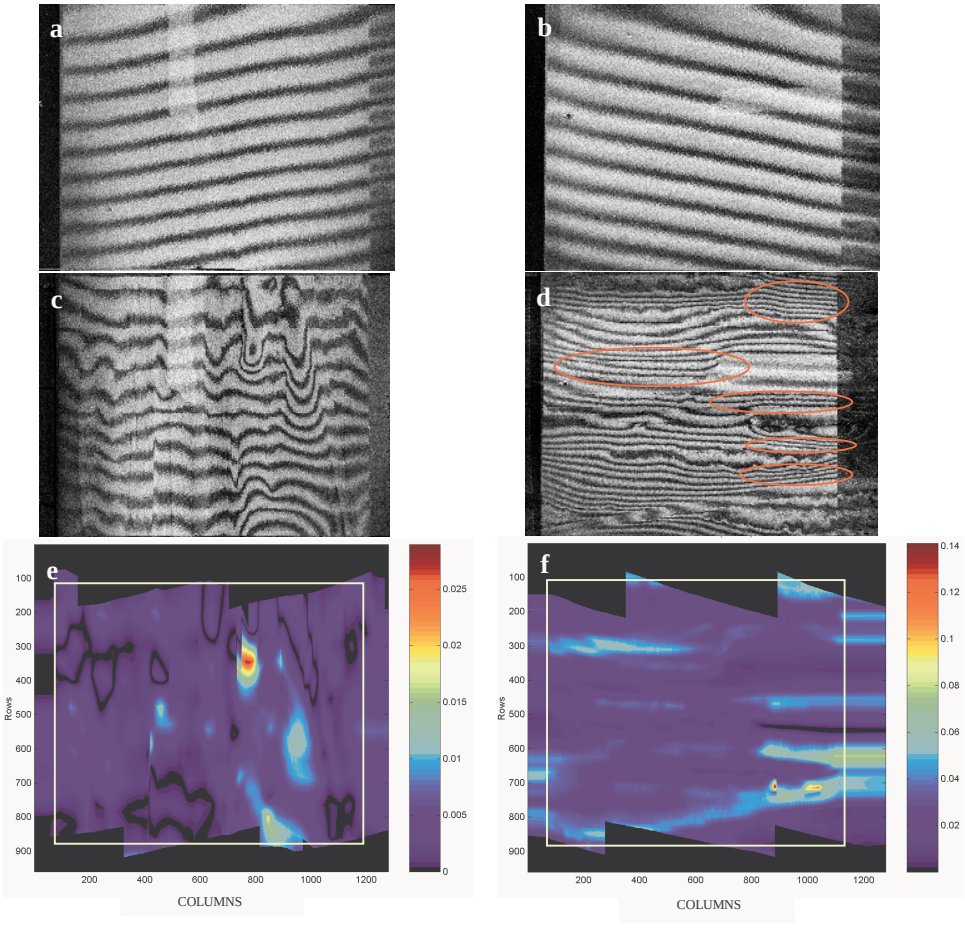

Figure 7. Moiré images from the second PWB at room temperature prior to thermal loading in the *u*-field orientation (a) and the *v*-field orientation (b), and at 177 °C for *u*-field orientation (c) and the *v*-field orientation (d), and strain maps (e) corresponding to (c) and (f) corresponding to (d). Areas of high strain are circled in red in image (d). The areas corresponding to the active gratings in (c) and (d) are indicated in yellow in (e) and (f) [7].

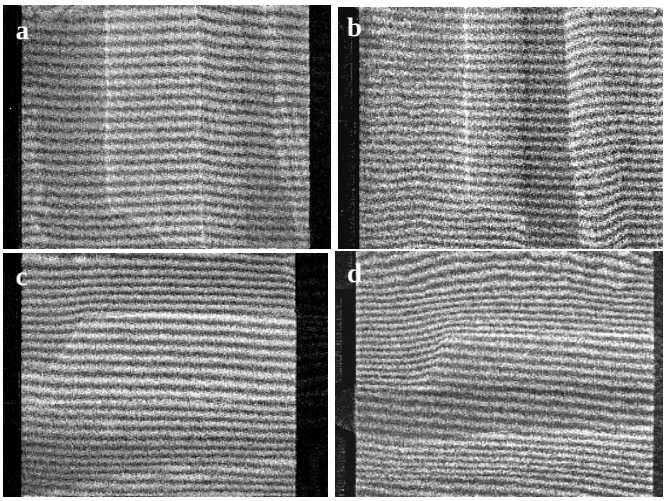

Figure 8. Moiré images taken at 177 °C from two different specimens from the same PWB: the *u*-field images of (a) the 0.5 mm termination and (b) of the 0.25 mm termination, and the *v*-field images of (c) the 0.5 mm termination and (d) of the 0.25 mm termination.